UNIVERSIDADE FEDERAL DO PARÁ
INSTITUTO DE GEOCIENCÎAS
FACULDADE DE METEOROLOGIA

VALERIA TAAKONDJO NAKALE

RADIATIVE EFFECTS OF AEROSOLS AND CLOUDS ON THE CO_2 FLUX IN CENTRAL AMAZON

BELÉM-PA
2022

VALERIA TAAKONDJO NAKALE

RADIATIVE EFFECTS OF AEROSOLS AND CLOUDS ON THE CO2 FLUX IN CENTRAL AMAZON

Course Completion work, presented as a partial requirement for obtaining a bachelor's degree in Meteorology, by Geociences Institute, Universidade Federal do Pará.

Area of expertise: Atmospheric Chemistry
Research Line: Climate and Functioning of Amazonian Ecosystems

Supervisor: Prof. Dr. Glauber Cirino - FAMET/IG/UFPA

BELÉM - PA

2022

Dados Internacionais de Catalogação na Publicação (CIP) de acordo com ISBD
Sistema de Bibliotecas da Universidade Federal do Pará
Gerada automaticamente pelo módulo Ficat, mediante os dados fornecidos pelo(a) autor(a)

N163e Nakale, Valeria Taakondjo.
Efeitos Radiativos de Aerossóis e Nuvens sobre o fluxo de CO2 na Amazônia Central / Valeria Taakondjo Nakale. — 2022.
57 f. : il. color.

Orientador(a): Prof. Dr. Glauber Guimarães Cirino da Silva
Trabalho de Conclusão de Curso (Graduação) - Universidade Federal do Pará, Instituto de Geociências, Faculdade de Meteorologia, Belém, 2022.

1. NEE. 2. Aerossois atmosfericas. 3. Balanço de carbono. 4. Amazonia. I. Título.

CDD 546.681

VALERIA TAAKONDJO NAKALE

RADIATIVE EFFECTS OF AEROSOLS AND CLOUDS ON THE CO2 FLUX IN CENTRAL AMAZON

Course Completion work, presented as a partial requirement for obtaining a bachelor's degree in Meteorology, Institute Geociences by Universidade Federal do Pará.

Area of expertise: Atmospheric Chemistry
Research Line: Climate and Functioning of Amazonian Ecosystems

Supervisor: Prof. Dr. Glauber Cirino - FAMET/IG/UFPA

Date of approval: 07/02/2022

Examination committee:

Prof. Dr. Glauber Guimarães Cirino da Silva - Supervisor
(Doctor – Climate and Environment)
Universidade Federal do Pará

Prof. Dr. Breno Cesar de Oliveira Imbiriba - Examiner
(Doctor – Physics)
Universidade Federal do Pará

Prof. Dr. Rafael da Silva Palácios - Examiner
(Doctor – Enviromental Physics)
Universidade Federal do Pará

I would like to dedicate this thesis to my loving mother.

ACKNOWLEDGEMENTS

I would like to thank my supervisor Professor Glauber, LABSAT for the resources provided, and PROPESP for the funding during the PIBIC project in 2019. I would also like to thank Professor Rafael for helping me in the process of doing this research, and most importantly UFPA, FAMET and the PEC-G program for the opportunity and the Namibian government for the scholarship opportunity that made all this possible.

“Motshitila mwaza ondjupa.”

(JOSEPH, 2009)

RESUMO

A floresta amazônica tem um papel crucial na formação do clima global, razão pela qual nas últimas décadas tem sido o foco de muitos estudos centrados em física atmosférica, alerta global e uso da terra florestal. Este trabalho tem como objetivo estudar a influência de nuvens e aerossóis na absorção de carbono na floresta intocada da Amazônia, contribuindo para o melhor entendimento do ciclo do carbono na Amazônia central. O local de estudo na área de observação da torre ATTO, 150 km a nordeste (em linha reta), ventos acima da cidade de Manaus (AM). A torre de observação utilizada para este estudo, atualmente coordenada pelo INPA (LBA), está localizada no município de São Sebastião do Uatumã, no estado do Amazonas. Os resultados mostraram que os maiores valores de NEE (valores mais negativos), são observados por volta das 10h00 - 14h00 durante o período de estação chuvosa, enquanto durante a estação seca, os maiores valores são registrados `as 09:00 - 15:00. Pode-se observar que existe uma relação linear entre AOD e irradiância relativa(f), irradiância relativa (f), diminui à medida que AOD aumenta, e os altos valores de longe encontram-se concentrados entre 0,2 e 0,4 dos valores MODIS AOD. A fração do PAR difuso aumenta quando há um aumento na AOD. Os maiores valores da fração do PAR difuso calculado concentram-se entre os valores de AOD de 0,2 e 0,4, e o NEE aumenta quando há aumento tanto no PAR-total quanto no f. Há uma diminuição da temperatura do ar à medida que a quantidade de nuvens e aerossóis aumenta, em valores de irradiância relativa entre 0,8-1,5 Wm^2, há uma diminuição da temperatura de topo do dossel com o aumento da nebulosidade e aerossóis. Concluímos que no ATTO, foi observado um aumento médio de 18 % e 25 % no fluxo de CO2 e NEE quando os valores de AOD variaram de 0,10 (fundo na Amazônia) a 0,30. O aumento de 18 e 25 % na NEE foi atribuído ao aumento da fração difusa da radiação solar em relação a sua fração direta, atribuível principalmente aos aerossóis biogênicos.

Palavras-chave: NEE; balanço de carbono; aerossóis atmosféricas; Amazônia.

ABSTRACT

The Amazon rainforest has a crucial role in shaping the global climate, which is why in recent decades, it has been the focus of many studies cantered around atmospheric physics, global warming, and forest land use. This work's main objective is to study the influence of clouds and aerosols on Carbon uptake in the pristine forest of Amazonia, contributing to a better understanding of the carbon cycle in central Amazonia. The study site is in the observation area of the ATTO tower, 150 km northeast (in a straight line), winds above Manaus (AM). The observation tower used for this study, currently coordinated by INPA (LBA), is located in the municipality of São Sebastião do Uatumã, in Amazonas. The results have shown that the highest values of NEE (more negative values) are observed around 10:00 am -14:00 during the wet season, while during the dry season, the highest values are recorded at 09:00 - 15:00. It can be observed that there is a linear relationship between AOD and Relative Irradiance(f), relative irradiance (f) decreases as AOD increases, and the high values of f are found concentrated between 0.2 and 0.4 of MODIS AOD values. The fraction of diffuse PAR increases when there is an increase in AOD. The highest values of the fraction of the calculated diffuse PAR are concentrated between AOD values of 0.2 and 0.4, and NEE increases when there is an increase in PAR-total and f. There is a decrease in air temperature as the number of clouds and aerosols increases, at values of relative irradiance between 0.8-1.5 Wm^2. There is a decrease in canopy top temperature with cloudiness and aerosols. We concluded that at ATTO, an average increase of 18 % and 25 % in CO2 flux and NEE was observed when the AOD values ranged from 0.10 (bottom in the Amazon) to 0.30. The 18 and 25 % increase in NEE was attributed to an increase in the diffuse fraction of solar radiation concerning its direct fraction, mainly attributable to biogenic aerosols.

Keywords: NEE; carbon balance; atmospheric aerosols; Amazon.

ILLUSTRATIONS

LIST OF ABBREVIATIONS

BC	Black Carbon
BrC	Brown Carbon
ITCZ	Inter-tropical Convergence Zone
LRT	Long Range Transport
LW	Long Waves radiation
MATLAB	MATrix LABoratory (programming and computing platform)
SW	Short Waves radiation
NEE	Net Ecosystem Exchange
PAR	Photosynthetically Active Radiation
VPD	Vapour Pressure Deficit
SZA	Solar Zenith Angle
AOD	Aerosol Optical Depth
MODIS	Moderate Resolution Imaging spectroradiometer
AERONET	Aerosol Robotic Network
Rh	Heterotrophic Respiration
NPP	Net primary Production
GPP	Gross Primary Production
EC	Eddy Covariance
Ra	Respiration

SUMMARY

1 INTRODUCTION

The Amazon rainforest has a crucial role in shaping the global climate, which is why in recent decades, it has been the focus of many studies centred around atmospheric physics, global warming, and forest land use. This study is no different, but we are focused more on aerosols and clouds over the Amazonia pristine forest. Andreae et al. (2015) stated that: the concentrations and types of aerosol particles over the Amazon basin exhibit enormous variations in time and space; this is due to the change in origins of the air masses arriving at ATTO throughout the year, as the Inter-tropical Convergence Zone (ITCZ) undergoes significant seasonal changes in the Amazon Basin, this results in pronounced differences in meteorological conditions and atmospheric composition.

Particle number concentrations that are very low in the wet season, averaging around 300 particles per cubic centimetre, can reach very high concentrations of around 30 000 particles per cubic centimetre in the dry season (PROCOPIO et al., 2004). Long-range transport (LRT) of trace gasses and aerosol particles also play an essential role in the composition of the Amazon rainforest atmosphere. For example: during the Amazonian dry season (August–November), the transport of African smoke from southern African savanna and shrubland fires is an essential source of aerosol in addition to regional emissions (ANDREAE et al., 1994).

Andreae et al. (2015) stated that Amazon aerosols are strongly influenced by seasonal variations in air mass origins, giving an example of the rainy season, when the biogenic aerosols over the Amazon are periodically overlapped by episodes of intense transatlantic transport, which bring both the dust of the Sahara and the smoke of forest fires; compared to the dry season, the dominant air masses source regions are to the east southeast, where biomass and fossil fuel combustion result in continuous and substantial production of polluting aerosols.

Large amounts of trace gasses, aerosols, ozone, and aerosol precursors are released into the atmosphere by intense biomass burning events that regularly take place in the vicinity of the Amazon Forest during the dry season (MALAVELLE et al., 2019). It is well known that aerosol particles affect the climate directly due to the change in the global radiation balance through the scattering and absorption properties of particles in the atmosphere that also influence cloud formation and its lifetime (GRIFFIN, 2013). Eltahir & Hamphries JR (1998) defined cloud cover as the fraction of the sky covered by clouds, regulating the amount of solar radiation reaching the earth’s surface traveling from the top of the atmosphere. Therefore,” it is

expected that clouds can have important ramifications on CO_2 exchanges between terrestrial ecosystems and the overlying atmosphere" (GU et al., 1999).

There is an expansion and intensification of agriculture, logging, and urban footprints, thus changing the Amazonian forest-river system, influencing, in the end, the hydrological cycle through the amount of water vapor released by the forest in the atmosphere, as well as cloud condensation nuclei, produced from forest emissions (ARTAXO et al., 2013).

The presence of clouds is an essential key in altering the surface radiation budget, as a higher amount of upwelling long-wave radiation from the ground is absorbed and re-emitted back to the surface (MYRBERG, 2015). The research carried out by Eltahir & Hamphries, (1998) found out that the net solar radiation is likely to decrease due to an increase in cloudiness, whereas net terrestrial radiation is likely to increase due to an increase in cloudiness. Hence, the net effect of clouds is to reduce net radiation; a 1 % increase in cloudiness induces a reduction in net radiation of ca 1 W/m^2. According to Collow; Miller, (2016), clouds reflect more short-wave radiation than absorbed, leading to significant changes at the boundaries but small changes within the column itself.

Clouds and aerosols together exert direct influence on the functioning of terrestrial ecosystems and are, therefore, expected to modify CO_2 exchanges in the biosphere atmosphere interface (CIRINO et al., 2014). A combination of modelling and observation-based studies have demonstrated that a shift in the distribution of light within the canopy can increase plant canopy uptake of atmospheric carbon dioxide (CO_2) with diffuse light (ZHU et al., 2019). An increase in the fraction of diffuse photosynthetically active radiation (PAR; 400–700 nm) (caused by clouds and aerosols) reaching plant canopies enhances photosynthesis and canopy-level productivity (RODERICK et al., 2001). Moreover, diffuse light increases the total canopy photosynthesis, referring to the diffuse fertilization effect. However, increased diffuse radiation might not be the only factor responsible for the enhanced ecosystem carbon assimilation observed under cloudy sky conditions (BALDOCCHI, 1997). Changes in other environmental factors, such as temperature and vapor pressure deficit, have also been identified as mechanisms through which cloud cover and diffuse light can alter CO_2 uptake by plant canopies (MIN, 2005).

Other studies have found that for a given irradiance level, overcast days generally have a higher NEE rate (in terms of the absolute value) than clear days (FAN et al., 1995), this is due to the amount of diffuse radiation available under these different sky conditions. We also must

consider how the solar elevation angles influence canopy photosynthesis. According to Ross, (1981), the solar elevation angle increases the proportion of the light reaching deeper canopies because of the reduced light extinction.

The net exchange of CO_2 in an ecosystem (Net Ecosystem Exchange - NEE) is the result of the different processes that regulate the flow of CO_2 in a forest (ROCHA, 2005), generally expressed by the sum of three terms: (i) CO_2 flow, calculated by the eddy correlation system; (ii) advective flux (Fadv), which expresses the horizontal mass transport, considered negligible if the location of the measurement is located over a vast area (homogeneous air sources) and (iii) by the term Fsto (storage), called term of storage. This last term considers the CO_2 storage effect within the forest canopy, usually calculated by measuring the CO_2 concentration in a discrete vertical profile at z height levels, with z thickness, from the ground surface to the point of eddy correlation measurements. In this work, the term Storage is calculated according to Araújo et al. (2010). All NEE analyses will be evaluated during the precise hours of the day, often between 09 -12 pm local time.

This study also looks at other factors such as PAR that can influence carbon uptake in the pristine Amazonia Forest. Min, 2005, stated that photosynthetically active radiation (PAR) is a fundamental variable affecting carbon uptake by ecosystems, not only the total amount but also its spectral distribution and its partitioning between direct and diffuse components, and in addition, stating that these aspects of PAR are strongly affected by clouds and aerosols.

1.1 Objetives

1.1.1 Geral Objetive

This work aims to study the influence of clouds and aerosols on Carbon uptake in the pristine forest of Amazonia, contributing to a better understanding of the carbon cycle in central Amazonia.

1.1.2 Specific Objectives

To achieve this work’s main objective, we must study the relationship between cloudiness and Carbon uptake at ATTO, study the relationship between Photosynthetically

active radiation and NEE, and analyse the influence of aerosols and clouds on other environmental factors such as air temperature, vapor pressure deficit and canopy temperature.

2 THEORETICAL REFERENCE

2.1 The Brazilian Amazon

The Amazonian rainforest is regarded as one of the primitive continental regions, and atmospheric aerosol particles over the region are expected to be affected minimally by anthropogenic activities, particularly during the wet season (MARTIN et al., 2010).

The Brazilian Amazon holds approximately 4 million km^2 of forests (HOUGHTON et al., 2000), covering approximately 75% of the total Amazonian area, (ARAGAO et al., 2014). Due to deforestation, about 18% of the original forest area has changed, mostly in southern and western Amazonia (OMETTO et al., 2005). The forests and soils of the Amazon basin also store a large amount of organic carbon (around 200 PgC), which may potentially be released to the atmosphere through the forest to pasture conversion or logging or because of biome changes (MALHI et al., 2008). There is also an expansion and intensification of agriculture, logging, and urban footprints, thus changing the Amazonian forest-river system

According to the Köppen Classification, in the Amazon occurs mainly both the Amw-type climate, which is characterized as tropical without season definite drought, as the Ami climate, which has a water deficit in the dry period that extends for up to 4 months. These are the types of hot, humid, and rainy weather conditions in the region, with an annual precipitation of 2200-3000mm and average temperatures of 22-27.9 ˚C (EMBRAPA, 2020).

During August, September, and October, the reduction in rainfall (> 25%) is very accentuated in those dry seasons and presents an increase in temperature > 2 ˚C, in addition to the length of the dry season being longer. This condition promotes an increase in the flammability of the forest and the mortality of trees typical of a humid tropical forest (INPE, 2021). There has been an increase in the population of Legal Amazonia from 8.2 million in 1972 to 28.1 million inhabitants in 2020, representing 13% of the Brazilian population. Nevertheless, the population density in the region is still low: 5.6 inhabitants per km^2. The Brazilian government has taken some measures to reduce deforestation and, in some cases, encourage reforestation in the past decades (ARTAXO et al., 2013), which has resulted in the curbing of deforestation in the Brazilian Amazon by 62% in 2010 relative to the 1990s mean decreased the Brazilian Amazon's deforestation contribution to global land-use carbon emissions from 17% in the 1990s and early 2000s to 9% by 2010 (ARAGAO et al., 2014).

Nobre et al. (2009) stated that the Amazonian forests play a critical role in regulating regional and global climate: although tropical forests pump latent heat into the atmosphere through intense evapotranspiration to balance the strong radiative heat at the surface, the complex interactions between climatic variables in the Amazon Basin have important implications for potential climate change at the local-global levels.

2.2 Atmospheric Aerosols

Wallace & Hobbs, (1995, p.169), referred to atmospheric aerosols as suspensions of tiny solid and/or liquid particles (excluding cloud particles) in the air with negligible terminal fall speeds. Their sources can be biological: when liquid and solid particles such as pollen, seeds, spores, and solid fragments from animals are released into the atmosphere, and when sea salts are ejected from the oceans. Another source of aerosols can also be the solid Earth when dust particles are transferred in the atmosphere by winds and earth turbulence. In addition, aerosols are also released from anthropogenic activities such as the burning of fossil fuels, industrial activities, and dust from roads. Lastly, some aerosol particles found in the Amazonia, are formed by the process of in situ condensations of gasses, such aerosols from the above sources are referred to as primary aerosols, and they are often larger than 1 micrometre.

Secondary aerosol particles are produced in the atmosphere from precursor gasses by condensation of vapours on pre-existing particles or by nucleation of new particles, and they consist of mixtures of compounds. The main components are sulphate, nitrate, and OC, this can also include the leading precursor gasses that are emitted from fossil fuel combustion, but fires and biogenic emissions of volatile organic compounds (VOCs), and their sizes can range from a few nanometres up to 1 micrometre (MYHRE et al., 2013).

In Amazonia, there can be found two types of aerosols, one of the main characteristics of aerosols that is crucial to this study is the aerosol optical depth, which according to NASA (2022), aerosol Optical Depth (AOD) is the measure of aerosols (e.g., urban haze, smoke particles, desert dust, sea salt) distributed within a column of air from the instrument (Earth's surface) to the top of the atmosphere (AOT), and according to Seinfeld and Pandis, (2006. p.981), it can also be defined as the product of coefficients per unit mass of aerosol and the aerosol mass concentration.

AOD also measures the spectral extinction of direct beam radiation according to the

application of Beer-Lambert–Bouguer law (HOLBEN et al., 1998) below.

$$V_\lambda = V_{o\lambda} d^2 \exp(\tau_\lambda m)\, t_\lambda \qquad (2.1)$$

where: V is solar irradiance, V_0 is the extra-terrestrial irradiance, m is the optical air mass, τ is the total optical depth, λ is the wavelength, d is the ratio average to the actual Earth-Sun distance and t_λ is the transmission of absorbing gasses.

Events with very high aerosol optical depths (τ>1.5at 500 nm) resulting from biomass burning are of great interest due to possible severe respiratory health impacts on portions of the population and due to other adverse effects, such as severe visibility reduction that may impede aviation operations (ECK et al., 2003).

Aerosol particles affect the climate directly due to the change in the global radiation balance through the scattering and absorption properties of particles in the atmosphere that also influence cloud formation and its lifetime (GRIFFIN, 2013). These particles also alter warm, ice, and mixed-phase cloud formation processes by increasing the number of droplet concentrations and the concentration of ice particles. They also decrease the precipitation efficiency of warm clouds and thereby cause an indirect radiative forcing associated with these changes in cloud properties (PENNER et al., 2001). In addition, the climate is directly affected by aerosols through reflecting or absorbing solar radiation and indirectly by aerosols acting as cloud condensation nuclei (CCN). Either way, the amount of solar radiation reaching the Earth's surface is reduced by aerosols (KULMALA et al., 2004).

Figure 1 - Energy budget components

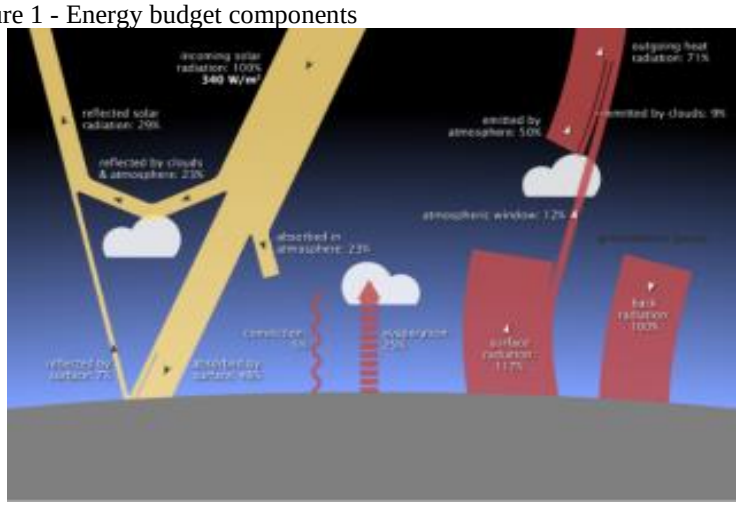

Source: Adapted from Andreae et al. (2015).

2.3 Carbon Balance

The carbon balance is governed by the following processes: the ones that release carbon in the atmosphere, which includes metabolic processes or physiological, photosynthesis, respiration, decomposition, and aquatic relationships, processes that include environmental determinants such as light, humidity, temperature, nominal CO_2, and nutrients. In addition, some processes make the Amazon a carbon sink. Such processes include disturbances and regeneration, including direct anthropogenic effects (e.g., deforestation for pasture), natural and indirect anthropogenic effects (e.g., fire) (HOUGHTON et al., 2009).

Figure 2 - The carbon cycle.

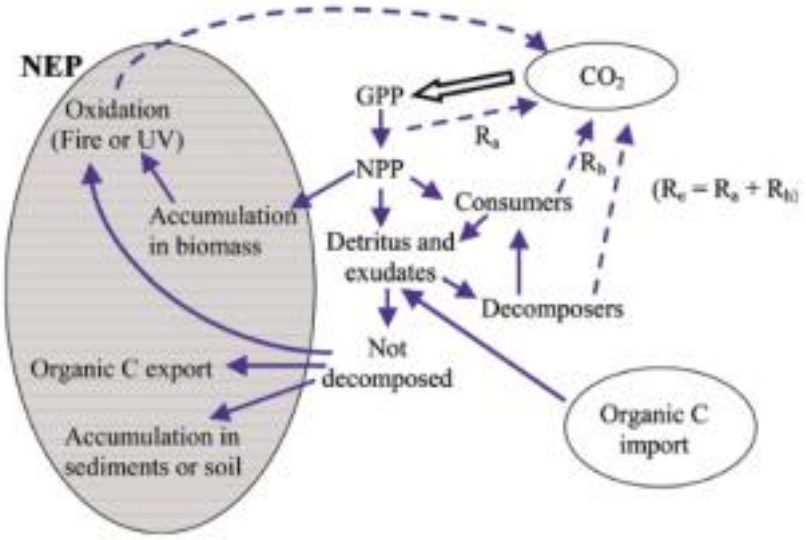

Source: Lovett, Cole e Pace (2006).

The figure above shows the fates of organic carbon (C) fixed in or imported into an ecosystem. Where R_e is the total ecosystem respiration, the sum of autotrophic respiration (R_a) and heterotrophic respiration (R_h). The shaded area contains the components of the system's NEP (Net Ecosystem Production). Accumulation in biomass represents all biomass (plant, animal, or microbial); the arrow is drawn from NPP (Net Primary Production) in this diagram because plant biomass accumulation is generally the largest biomass term. NPP, net primary production; NEP, net ecosystem production; GPP, gross primary production; CO_2, carbon dioxide; UV, ultraviolet (LOVETT; COLE; PACE, 2006).

The Amazon appears to be a significant source of CO_2 for the atmosphere, and this is

due to deforestation of between 15 and 20 thousand km2 per year only in the Brazilian Amazon (INPE, 2001; NOBLE & NOBLE, 2002). Measurements of atmospheric CO_2 provide such a constraint on NEE (BOUSQUET et al., 2000). With reference to Cirino et al. (2014), deforestation and reforestation in the Amazonia have played a significant role in the forest's net carbon source of 0.14-0.35 PgC and 0.2-0.8 PgC released from forest fires.

There is a strong indicated influence of extreme climatic events and land-use change on the current carbon cycle of Amazonia, and they have the potential to cause significant global climate impacts (ARAGAO et al., 2014). The net carbon budget of a forest is defined as a fine balance between processes of carbon acquisition (photosynthesis, tree growth, forest aging, carbon accumulation in soils) and processes of carbon release (respiration of living biomass, tree mortality, microbial decomposition of litter, oxidation of soil carbon, degradation, and disturbance) (MALHI; BALDOCCHI; JARVIS, 1999), more information can be found in Kirschbaum et al. (2001).

Two critical environmental factors are affecting the stability of the Amazonian carbon cycle: climate variability and human activities (ARAGÃO et al., 2014). More information about the Amazonian carbon cycle can be found in Aragao et al. (2014).

2.4 Effects of aerosols on the balance of carbon /flux

Previous studies on aerosol's influence on ecosystem production have found that fire aerosols can promote photosynthesis by enhancing diffuse light, reduce photosynthesis due to light attenuation associated with increasing aerosol burden, and affect ecosystem productivity indirectly by adjusting surface climate (LI, 2020).

Aerosols from released biomass burning also contribute to the formation of a large amount of ozone, and according to Bulbovas et al. (2007), the ozone levels observed in recent studies, which are sometimes higher than 100 ppb, can play an essential role in the primary productivity of Amazonian vegetation because some species and cultivars are sensitive to high levels of ozone.

High cloud cover leads to strong decreases in photosynthesis up to the point where NEE approaches zero. The observed increase in NEE is attributed to an enhancement in the diffuse fraction of photosynthetic active radiation (PAR). With reference to Cirino et al. (2014), the enhancement in diffuse PAR can be done through increases in aerosols and/or clouds. The

cooling of anthropogenic aerosols has different impacts in different latitudes but overall increases the global land carbon sink. The dominant role of diffuse radiation changes found in this study implies that future aerosol emissions may have a much stronger impact on the carbon cycle through changing radiation quality than through changing climate alone (ZHANG et al., 2021).

3 METHODOLOGIES

3.1 Location and description of area of study

Micro-meteorological observations and measurements were carried out in a primary forest ecosystem in central Amazonia. The study site is in the observation area of the ATTO tower, 150 km northeast (in a straight line). The observation tower used for this study, currently coordinated by INPA (LBA), is located in the municipality of São Sebastião do Uatumã, in Amazonas (W 2° 34’ 20” S, 57° 52’ 17” W). The Amazon Tall Tower Observatory (ATTO) consists of several observatory towers built in the middle of the Amazon rainforest for a continuous and detailed study of biota–atmosphere interactions (WU et al., 2019).

Figure 3 - Map showing the location of ATTO in the Uatumã forest

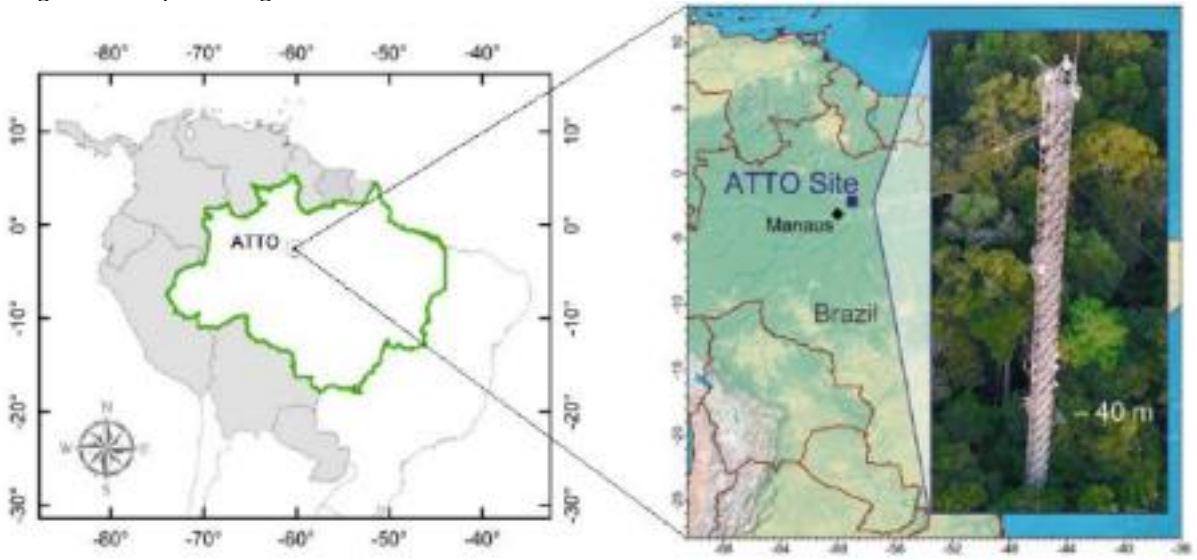

Source: Pfannerstil et al. (2018).

The Amazon Tall Tower Observatory (ATTO) was installed about 150 km north-east of the city of Manaus, in an untouched rainforest region in the central Amazon Basin (ANDREAE et al., 2015). It was built to provide innovative discoveries and a foundation for improving climate models. With a height of 325 meters, the design allows the tower to extend high above the rainforest and collect information from an area of approximately 100 square kilometres of the world’s largest continuous rainforest area (MANZI, 2015). In addition, Andreae et al. (2015) reported that an ecological survey including biodiversity assessment was

carried out in the forest region around the site, in addition to meteorological and micro-meteorological measurements including temperature and wind profiles, precipitation, water and energy fluxes, turbulence components, soil temperature profiles, and soil heat fluxes, radiation fluxes and visibility are also taken at ATTO.

The municipality has the type of climate Af, equatorial humid, according to Köppen - Geiger. The monthly records have a maximum temperature of 38 ºC and a minimum of 20.5 ºC, relative humidity of 80 percent, and almost year-round rainfall; the highest is recorded in December and the dry month in August. The region has two distinct seasons, the rainy season between December-April and the dry season between July-October. The wind is predominantly from the east direction, and the average speed is 24 and 28 km/h. Cloud types are large, vertically developing cumulus-nimbus that can reach a height of 500 - 1000m.

3.2 Data and instrumentation

All the experimental measures necessary are public and granted directly by the LBA DIS (Data Information System), which currently concentrates the data generated in the various Flow Towers implemented in the Amazon. LBA's flow towers currently operate a wide variety of sensors for direct measurement of micro-meteorological variables and trace gasses, such as temperature, humidity, solar radiation, rain, wind direction and speed, CO_2, CO, CH_4, H_2O and countless other variables, as shown in the table below (Table 1).

Turbulent exchange fluxes of H_2O and CO_2 as well as surface boundary layer stability is measured within and above the canopy using the eddy covariance (EC) technique. Three-dimensional wind and temperature fluctuations were measured by sonic anemometers at 81, 46 and 1.0 m. CO_2 and H_2O fluctuations are detected by three fast response open-path CO2 / H2 O infrared gas analysers installed at a lateral distance of about 10 cm from the sonic path. The high-frequency signals are recorded at 10 Hz by CR1000 data loggers (ANDREAE et al, 2015).

The data period selected for this study was from March 5th to May 31st (rainy month), January 1st, 2012 to December 31st, 2016. Statistical analyses for the calculation of the NEE will be performed during representative months of the rainy season (Feb-Apr) and the dry season (Aug-Oct). We will analyse the components of the NEE for the carbon balance under different coverage and cloud conditions; the calculation of cloud cover (cloud cover fraction) will be expressed in terms of atmospheric transmissivity, following the criteria established by

(GU et al. 1999). Two transmissivity ranges will be considered: less than 0.30 and larger than 0.70. We will use the same procedure as Silva et al. (2002), using these bands to determine when the sky conditions at the experiment site are (1) cloudy and (2) cloudless.

Table 1 - List of measurements done at ATTO.

Measurements	Unit	Instruments	Meas.height(m)
Short-wave radiation (incoming and reflected)	Wm^{-2}	Pyranometer (CMP21, K& Z)	75
Long-wave radiation (atmospheric and terrestrial)	Wm^{-2}	Pyrgeometer (CGR4, K & Z)	75
PAR (incoming and reflected)	$Mmolm^{-2}\,s^{-1}$	Quantum sensor (PAR LITE, K & Z)	75
Net radiation	Wm^{-2}	Net radiometer (NR-LITE2, K & Z)	75
Air temperature and relative humidity	°C & %	Termohygrometer (CS215, Rot.)	53
Atmospheric pressure	hPa(mb)	Barometer (PTB101B, Vaisala)	75
CO_2 flux	$\mu molm^{-2}s^{-1}$	Eddy covariance system	81
CO_2 storage	ppm	IRGA(LLI-7500, LL-COR Inc.)	12, 24, 37, 79
Aerosol Optical Depth	-	MODIS/AERONET	80

Source: Andreae et al. (2015).

3.3 Aerosol Optical Depth

Aerosol optical depth (AOD) was calculated from irradiance measured with the MODIS (Moderate Resolution Imaging Spectro-radiometer) sensor onboard the Terra and Aqua satellites. Remotely sensed aerosol optical depth measurements at 550 nm are taken from two sources, the MODIS instrument on the Aqua and Terra platforms (MODIS Atmospheric Products, MOD/MYD 04L2), sweeping 2330 km-wide viewing swath and sees every point on our world every 1-2 days in 36 discrete spectral bands; and from the solar radiometer network AERONET (Aerosol Robotic Network) (HOLBEN et al., 1998). Palácios et al. (2019) also indicated that these measurements allow the near real-time monitoring of the optical thickness of the aerosols, precipitating water column, and particle size distribution, among other physical and optical properties of aerosols. The level of processing of the data used in this study is level 2.0. At the 2.0 level, a cut is made for the optical depth of the aerosol in the channel of 550 nm (AOD 550 nm). Direct solar measurements have a field of view of 1.2° for eight spectral bands

centred at 340, 380, 440, 500, 670, 870, 940 and 1020 nm, determined by rotational interference filters located within the sensor. Each measurement takes approximately 10 s (ANDREAE et al., 2015).

3.4 Methods

3.4.1 Data analysis

Data analysis was done with MATLAB's programming platform; for better analysis, firstly, the short and long-wave radiation data were separated into three groups, the rainy, dry, and transition seasons. The radiation balance for the three different seasons was calculated. The clearness index was also determined, a procedure that facilitated the study and identification of the effects of clouds or their absence on the radiation balance. For measurements of cloudiness or the presence of clouds in the sky, no direct observations were made, but instead, we used a method that was used by Gu et al. (1996). To calculate cloudiness, we use the clearness index, which is defined as the ratio of global solar radiation received at the Earth's surface to extra-terrestrial irradiance in a plane parallel to the Earth's surface (GU et al., 1999), and IT is expressed by:

$$k_t = \frac{S}{S_e} \tag{3.1}$$

where,

$$S_e = S_c \left[1 + 0.033 \times \cos\left(\frac{360td}{365}\right)\right] \sin\beta \tag{3,2}$$

Where k_t denotes the clearness index, S_e denotes the extra-terrestrial irradiance in a plane parallel to the earth's surface (Wm^{-2}), S_{sc} is the solar constant ($370Wm^{-2}$), β is the solar elevation angle and td denotes the day of the year.

The relationship between kt and relative irradiance (r) is given by the equation below:

$$r = \frac{S}{S_o} = \frac{k_t \times S_e}{k_{to} \times S_e} = \frac{k_t}{k_{to}} \quad (3.3)$$

k_{t0} is the clear-sky clearness index. There is a strong relationship between the clearness index and solar elevation angles and cloudiness, and according to Gu et al., (1999), under clear skies, the clearness index increases with solar elevation. And the following cubic polynomial to fit the clear-sky clearness index k_{t0} from sinβ (CIRINO et al., 2014).

$$k_{to} = a_1 \times \cos^3(z) + a_2 \times \cos^2(z) + a_3 \times \cos(z) + a_4 \quad (3.4)$$

Where a_1, a_2 and a_3 are site-specific regression coefficients for morning and afternoon. Figure 20 in Annex 1 shows the table with fitted calculated values of a_1, a_2, and a_3 with the clearness index for more information about the calculated regression coefficients of relationships between clear-sky irradiance S0 and solar zenith angle cos(z) as well as relationships between clear-sky clearness index and solar zenith angle cos(z) for the morning and afternoon periods by Cirino et al. (2014). The graph below (scatter plot) shows the relationship between the clear-sky clearness index(k_t) and the solar zenith angle(z).

Figure 4 - Scatter plot and regressions between clear-sky clearness index and cosine of soar zenith angles.

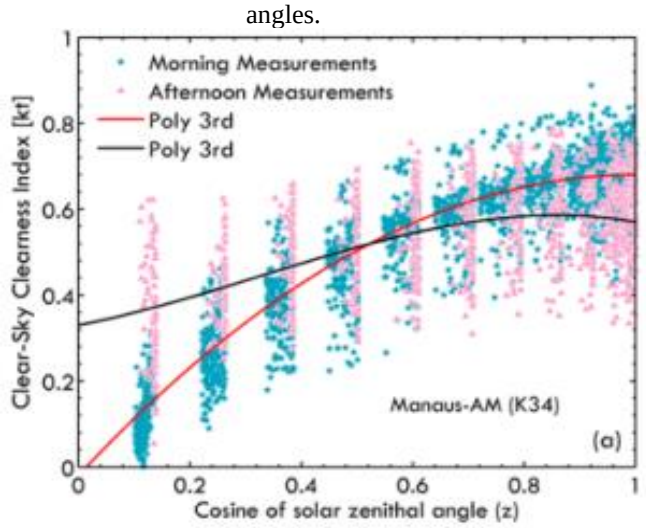

Source: Cirino et al. (2014).

3.4.2 Defining clear sky

As was done in Gu et al. (1999), we defined the clear sky as the basis of comparison in this study. The clearness index values were plotted against the radiation balance values during separate seasons, e.g., dry, wet, and the transition season. This provides a basis for the comparison of NEE behaviour for" clear-sky days" vs. aerosol and cloudy days (CIRINO et al., 2014).

Cloud conditions were also separated into clear, partially cloudy, and cloudy skies, which made it easier to study and determine the degree to which clouds affect the radiation flux on the earth's surface and how this affects positively or negatively in different processes, such as NEE of CO_2, and all hydrological processes. With reference to Eltahir & Hamphries, (1998), clouds absorb a significant amount of the upward stream of terrestrial radiation and emit radiation back to the surface. Consequently, clouds are significant in determining downward terrestrial radiation and net terrestrial radiation at the surface. As terrestrial and solar radiation are heavily dependent on the cloud field, clouds play an essential role in the surface energy balance.

To quantify the specific influence of clouds on NEE, first, the NEE behaviour on days with minimal cloud cover was determined using the clear day separation method of Gu et al. (1999), this provides a basis for comparing NEE behaviour for clear sky days (AOD~ 0.10) vs. aerosol and cloudy days (CIRINO et al., 2014).

3.4.3 Calculation of net ecosystem CO_2 exchange (NEE)

According to Oliveira et al. (2018), the net exchange of CO_2 (NEE) results from the balance between the following processes: heterotrophic respiration (Rh) and net primary production (NPP) - Heterotrophic respiration is the carbon lost by the organisms in ecosystems other than plants. NPP consists of gross primary production (GPP) minus the amount of carbon that the plants themselves breathe (Ra). Gross primary production (GPP) refers to the total amount of carbon fixed in the photosynthesis process by plants in one ecosystem (KIRSCHBAUM et al., 2001). The relationship between the above-mentioned processes is shown in the equations below.

$$NEE = NPP - Rh \quad (3.5)$$

$$NPP = GPP - Ra \quad (3.6)$$

$$NEE = GPP - Ra - Rh \quad (3.7)$$

Measurements for turbulent exchange fluxes of CO2 are made within and above the canopy using the eddy covariance (EC) technique (ANDREAE et al., 2015). Micro meteorological sensors distributed vertically along the tower are essential for NEE calculations using continuous measurements of the CO2 profile between the ground (z 0) and the top of the tower (z). Under these conditions (Richardson & Hollinger, 2005), the NEE can be approximated by Artaxo et al. (2013),

$$NEE \cong FuxC + SCO_2 \quad (3.8)$$

FluxC is the turbulent flux of CO_2 above the canopy, and SCO_2 which was used in this study) represents carbon storage (Stg) the non-turbulent storage term, defined as the temporal variation of the CO_2 concentration measured in a vertical profile from the soil surface to the height of eddy correlation measurements. The non-turbulent storage SCO_2 is calculated using the formula:

$$sco_2 \cong [\frac{P(air)}{RT(air)}] \int_0^z \partial \frac{[CO_2]}{\partial t} dz \quad (3.9)$$

Where R is the ideal gas constant in ($N\mu mol^{-1}K^{-1}$) and t represents the time in seconds.

3.4.4 Procedure for quantifying aerosol and cloud effects on NEE

The concept of relative irradiance, f, was used to determine the reduction of incident solar irradiance due to clouds and aerosols and associate this with the changes in NEE, which also changes with temperature and variations of relative humidity (CIRINO et al., 2014). The relative irradiance(f) (in the equation below) was calculated to quantify the aerosol and cloud effects on the NEE and to produce a measurement of the reduction in the total downward solar flux caused by the presence of aerosol particles and clouds in the atmosphere, compared with the clean atmosphere (OLIVEIRA et al., 2007).

$$f \cong \left(\frac{(SW_{inc})(AOD,coudiness)}{(SW_{inc})(AOD{\sim}0.10.cloudless)} \times 100\right) \quad (3.10)$$

Here, S (Wm^{-2}) is the total incident solar radiation measured at the surface for a given time (with or without the presence of aerosols and clouds), and S_0(Wm^{-2}) is the expected total incident solar irradiance at the surface in a cloudless atmosphere with an aerosol optical depth of 0.10 at 550 nm (GUYON et al., 2003).

Since this study is heavily based on the calculations done by Cirino et al. (2014), it is stated that to observe only the aerosol effects on the solar irradiance flux (computed from f), and consequently, on the NEE measurements, the aerosol effects have to be isolated from the cloud effect.

3.4.5 Determination of NEE on clear skies days

In this section, we are going to make observations for only the aerosol effect on the solar irradiance flux (computed from f), and consequently, on the NEE measurements, the aerosol effect has to be isolated from the cloud effect. Measurements were classified as affected only by aerosols if they were performed under cloudless conditions (OLIVEIRA et al., 2007).

The NEE observed on clear days was also used to compare cloudy days and days with high aerosol loading. As in the study by Cirino et al. (2014), this study similarly used the

influence of aerosols and clouds on carbon uptake, which is analysed mainly in terms of variations in NEE and environmental factors through their impact on f, observed NEE on clear days (AOD < 0.1 and cloud-free) was also used as a basis of comparison for cloudy days and days with high aerosol loading. Changes in the observed NEE relative to NEE with clear skies were used to determine the percentage effect of aerosols and clouds on the NEE (% NEE). The % NEE was calculated by the following relationship (OLIVEIRA et al., 2007):

$$\%\mathrm{NEE} \cong \frac{\mathrm{NEE_z} - \mathrm{NEE_{csky}}}{\mathrm{NEE_{csky}}} \tag{3,11}$$

In this case, NEE(z) represents a measure of NEE under a given sky condition throughout the day, and NEE_{csky} is the NEE calculated under sky conditions with low aerosol loading in the atmosphere and minimal cloud cover (f ~1.0, AOD ~0.10).

3.4.6 Deriving PAR and diffuse PAR

We studied other factors that influence the forest's light use efficiency, specifically PAR and diffuse PAR. The diffuse PAR was calculated by coupling several relationships reported in the literature of GU et al. (1999) and Cirino et al. (2014), and it is given by:

$$\mathrm{PAR_f} = \left[\frac{[1+03(1-q^2)]q}{1+(1-q^2)\cos^2(90-z)\cos^3 z}\right] \times \mathrm{PAR_t} \tag{3.12}$$

Where PAR_f is the diffuse PAR radiation flux (μmol photon $m^{-2}s$), PAR_t is the total PAR and the parameter "q" is a proportionality coefficient used to denote the ratio of total diffuse radiation to a given amount of irradiance (S) that reached surface under a given sky condition (Wm^{-2}) (CIRINO et al., 2014). The proportionality coefficient (q) is calculated using the expression below:

$$q = \frac{S_f/S_e}{k_t} \tag{3.13}$$

In this equation, Sf denotes the total diffuse radiation received on the horizontal plane at the earth's surface, while Se denotes the solar irradiance and kt is the clearness index (CIRINO et al., 2014).

We have evaluated the influence of diffuse PAR in the light use efficiency (LUE) of the forest, using the equation below:

$$\mathrm{LUE} = {}^{\mathrm{NEE}}/_{\mathrm{PAR_t}} \tag{3.14}$$

Most importantly, to evaluate the effect of diffuse PAR radiation (PAR_f) on LUE, it is common to define the parameter Df, which is the ratio between (PAR_f) and total PAR (PAR_t) (CIRINO et a., 2014):

$$\mathrm{D_f} = \mathrm{PAR_f}/\mathrm{PAR_t} \tag{3.15}$$

3.4.7 Influence of aerosols and clouds on the air and canopy top temperature as well as VPD

No direct measurements for the canopy top temperature were made, but it was calculated/derived from the Stephen Boltzmann's equation, using the long wave radiation measured by the pyrgeometer. The equation used is as follow:

$$\mathrm{T_c} = (\mathrm{L}\uparrow/\sigma\varepsilon)^{0.25} \tag{3.16}$$

Where σ is the Stephen Boltzmann's constant, ($5.670\times10^{-8}\mathrm{Wm^{-2}K^4}$) and ε is the emissivity, with the assumed value of 0.98. The same procedure was used by (CIRINO et al., 2014).

4 RESULTS AND DISCUSSION

In this chapter, we are going to analyse the influence of clouds and aerosols on NEE, focusing specifically on the following: the influence of aerosols on PAR and relative irradiance, and the effect of PAR (diffuse) radiation on the light use efficiency (LUE) through the forest, and the influence of other environmental factors on the relative irradiance. Oliveira et al. (2014) stated that in Amazonia, most NEE measurements are affected all over the entire year, even in the dry season, since clouds are present most of the time and there is frequent precipitation.

4.1 Diurnal cycle of net ecosystem exchange

The diurnal cycle of NEE comprises positive values occurring during the night period indicating the release of CO_2, mainly by the respiration process of the ecosystem. On the other hand, the negative values that occur during the daytime indicate the absorption of CO2 through photosynthetic activity carried out by vegetation (SILVA, 2010). The negative and positive values are also due to photosynthesis being higher than respiration during the day and vegetation respiration being high during the night.

Figure 5 shows the diurnal cycle of NEE at ATTO during the dry and wet seasons, respectively. The highest absolute values of NEE (more negative values) are observed in the wet season (more negative values). The more negative values of NEE are observed around 10:00 -14:00 during the wet season. During the dry season, the highest values are recorded at 09:00 - 15:00. The highest absolute value of NEE during both seasons was recorded just above $-30 \mu molm^{-2} s^{-1}$.

Figure 5 - Diurnal cycles of NEE during the wet and dry season

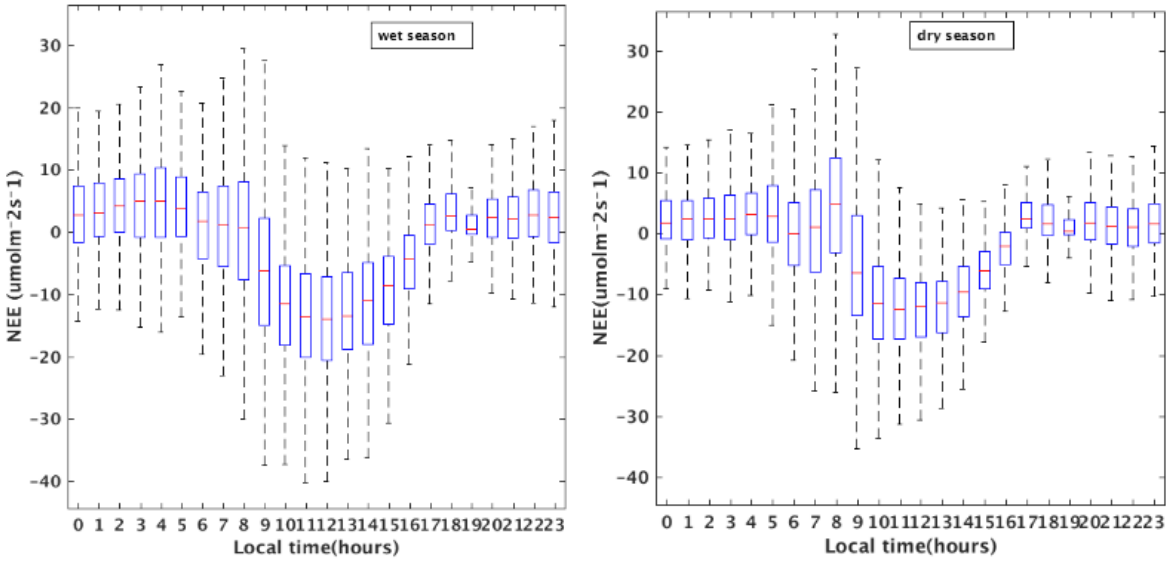

Source: Cleverly et al. (2016)

The high variation of NEE during the wet season can be attributed to rainfall. During periods of rainfall abundance, there are more nutrients available in the soil, resulting in a faster, more efficient absorption by plants, increasing leaf development and productivity (CLEVERLY et al., 2016).

4.2 MODIS and AERONET AOD for ATTO

Figure 6 shows the time series of AOD of 550 nm in the central Amazon at the ATTO site between 1999 and 2018. AERONET data observations only started in 2016, as indicated by the graph. Therefore, values between 2012 and 2016 are between 0 and 0.8. Although, in other studies, such as Cirino et al. (2014), it has been observed that AOD values tend to be high during the dry season when biomass burning is prevalent. Also, due to the long-range transport of particles, it has been indicated that the AOD values remain low during the wet season, and such values are similar to the typical background values of aerosols found in the Amazon.

Figure 6 - Time series of AOD from 1999 to 2018 estimated by MODIS and AERONET.

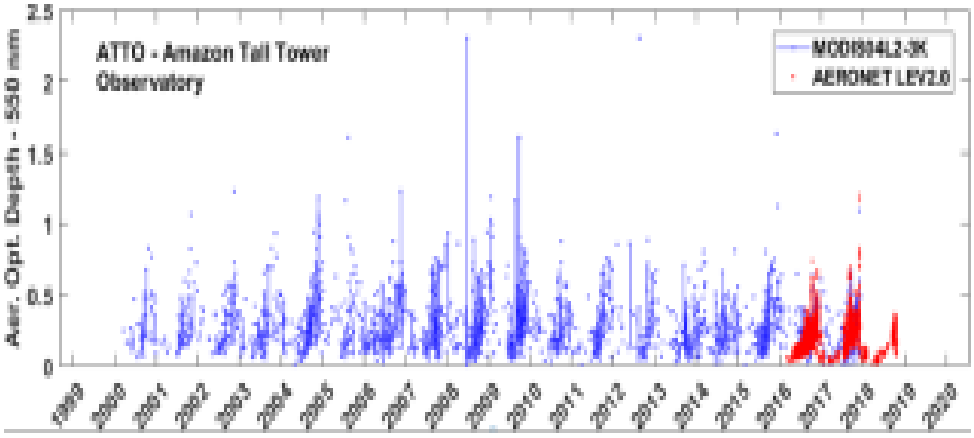

Source: Own figure

4.3 The influence of aerosols and clouds on PAR radiation and relative irradiance

In this section, we observe the influence of aerosols and clouds on relative irradiance. Figure 7 below shows the behaviour of relative irradiance f as a function of AOD under minimal cloud effects; the graph also represents the effects of aerosols on the relative irradiance, where it can be observed that there is a poor linear relationship between AOD and Relative Irradiance(f), with R^2 of 0.10, which is a poor linear relationship but better than no relationship at all, shown by pval<0.01. Relative irradiance (f) decreases as AOD increases, and the high values of f are found concentrated between 0.2 and 0.4 of MODIS AOD values. For cos(z) values between 10 and 65°, we can observe a decrease in f values of 16% when AOD values varied from 0-1.

Figure 7 - The relationship between relative irradiance f and MODIS AOD for ATTO.

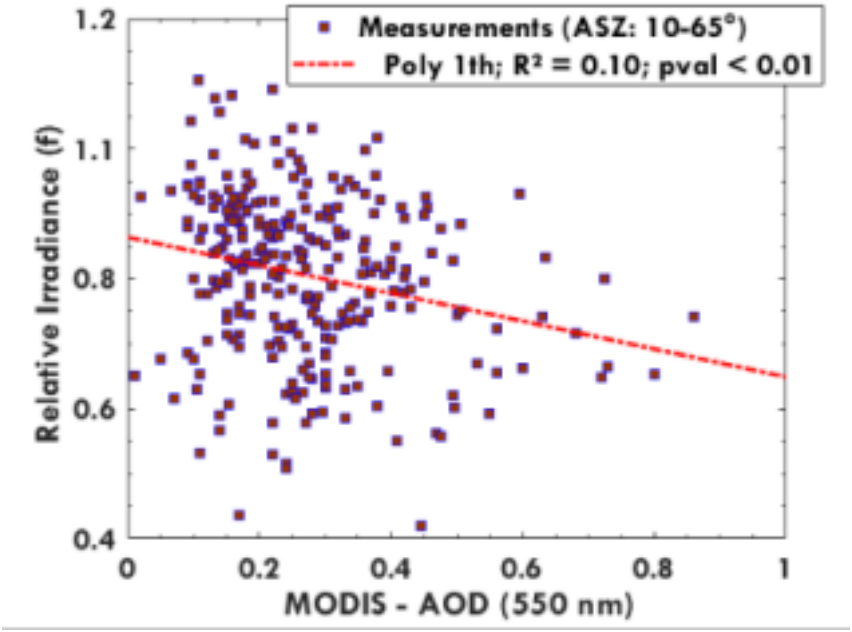

Source: Own figure

Figure 8 shows the scatter plot for the relationship between a fraction of calculated diffuse PAR, as a function MODIS AOD, and we can also observe a poor linear relationship between the fraction of diffuse PAR and AOD values, with R^2 of 0.11 and a better relationship given by pval<0.01. The fraction of diffuse PAR increases when there is an increase in AOD. The highest values of the fraction of the calculated diffuse PAR are concentrated between AOD values of 0.2 and 0.4. These results are significant because diffuse PAR penetrates more efficiently in the canopy and contributes to an increase in carbon uptake (CIRINO et al., 2014). For cos(z) values between 10 and 65°, there is an increase of 22% in f values when AOD values vary from 0-1.

Figure 8 - The relationship between the fraction of diffuse PAR and MODIS AOD for ATTO.

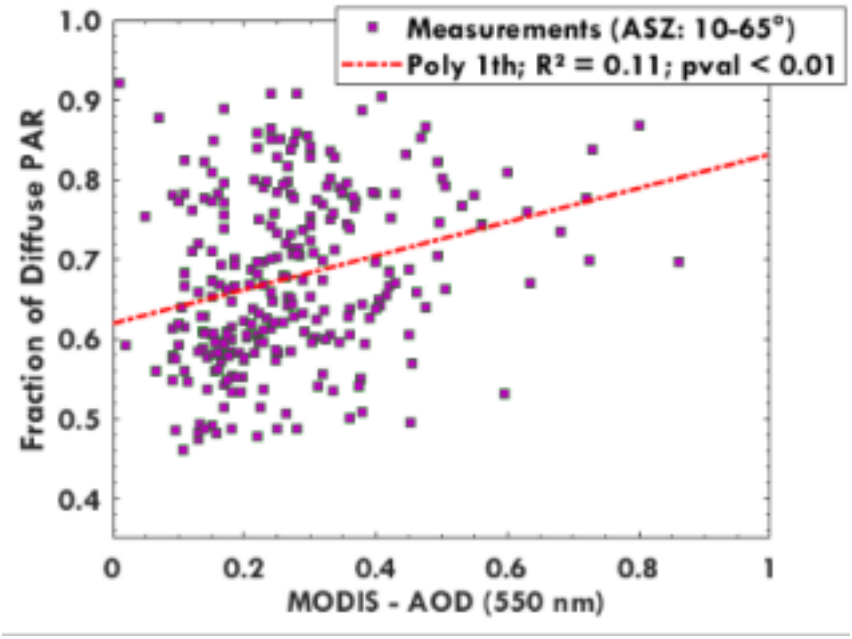

Source: Own figure

The figure below, figure 9, shows the relationship between the total PAR and relative irradiance f. We can observe a linear relationship between f and PAR-total. There is an increase in PAR-total as f increases; the NEE increases when there is an increase in both PAR-total and f. For cos(z) between 10-65°, for f values varying from 0.8-1.0, there is an increase of 11% in PARtotal. There is also a decrease in PAR total as the sky changes from clear to cloudy (f 1.0 to f<0.10).

Figure 9 - The relationship between total PAR and relative irradiance for ATTO.

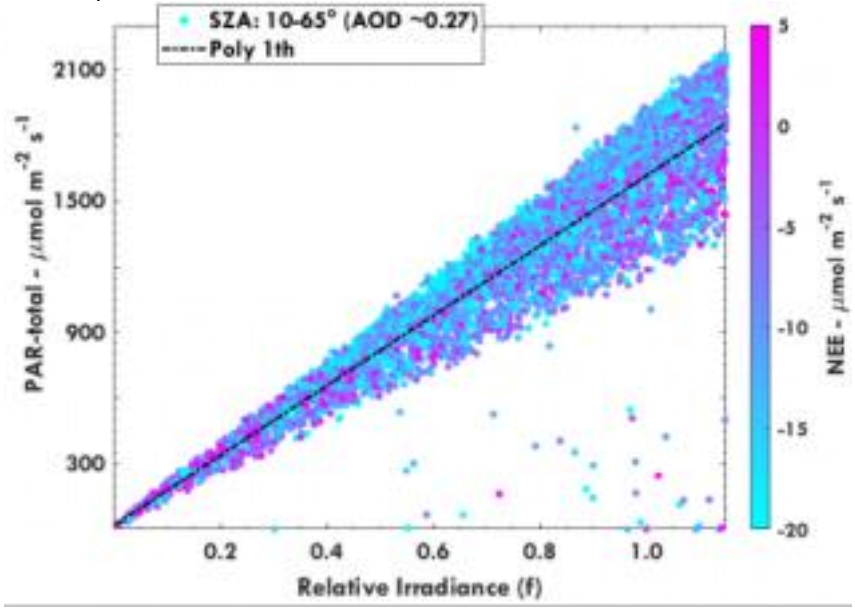

Source: Own figure

Figure 10 shows the relationship between diffuse PAR and relative irradiance. There is an increase of 45% from 500 µmolm^{-2}s^{-1} in diffuse PAR when relative irradiance decreases from 1.2 to 0.8. The maximum diffuse PAR was observed between f values of 0.6 and 0.8. The relationship shown between relative irradiance and NEE is consistent with that of Oliveira et al., 2007, where it can be observed that with the increase of the number of aerosol particles in the atmosphere (a reduction of f), the NEE values increase (gets more negative), it is also stated that for similar observation in the case of the predominantly cloud presence, the maximum (more negative) value of the NEE measurements does not occur on clear-sky days (f=1.0), but occurs with relativity high aerosol loading in the atmosphere.

Figure 10 - The relationship between PAR-diff and relative irradiance with NEE for the solar zenith angle of 10-60 degrees and with AOD of 0.27.

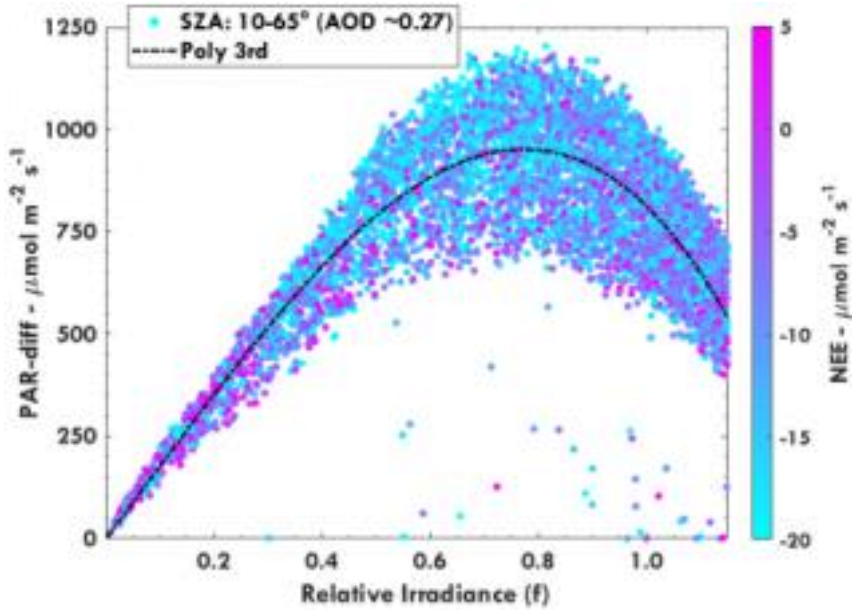

Source: Own figure

4.4 The effect of PAR (diffuse) radiation on the use of light efficiency (LUE) through the forest

In figure 11, we have the relationship between NEE and total PAR in the presence of clouds and aerosols and the relative irradiance for the solar zenith angles between 10 and 65 °. We can observe that with an increase in NEE (more negative values) with an increase of total PAR, and a decrease in NEE (more positive values) as total PAR decreases, the same behaviour is observed with an increase in aerosols and clouds as total PAR increases. In contrast, the relative irradiance increases with an increase in total PAR, and (relative irradiance increases with an increase in clouds and aerosols). It can also be said that there is great assimilation of carbon with the increase in total PAR, with the maximum value of 1200 and NEE value of -40 $\mu mol^{-2}s^{-1}$.

There is a large scattering of NEE with clouds and aerosols at lower values of total PAR and small scattering for NEE with high values of total PAR, with lower values of relative radiance found in the presence of clouds and aerosols and high values found in the presence of small scattering of NEE and clear sky-like conditions.

Figure 11 - NEE as a function of total downward PAR radiation, evaluating the relative irradiance in the observed conditions for ATTO, for the solar zenith angles between 10 and 45°, the green and blue colours represent the relative irradiance.

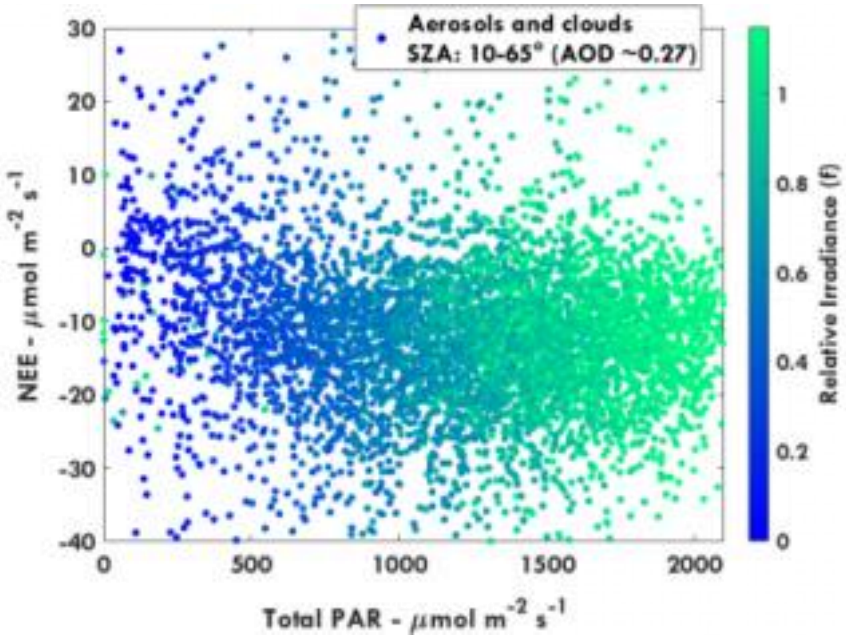

Source: Own figure

Figure 12 below shows the relationship between the NEE and the calculated fraction of diffuse PAR. This relationship represents photosynthetic efficiency, which is related to the ability of the canopy to convert solar energy into biomass (CIRINO et al., 2014). It can be observed from the graph that the LUE is low, with values varying below 0,02%.

Figure 12 - Scatter plot of relative irradiance observed from the relationship between the fraction of NEE and total PAR with the fraction of diffuse radiation, for ATTO site for the period of 1999-2019, for the solar zenith angles between 10 and 65°.

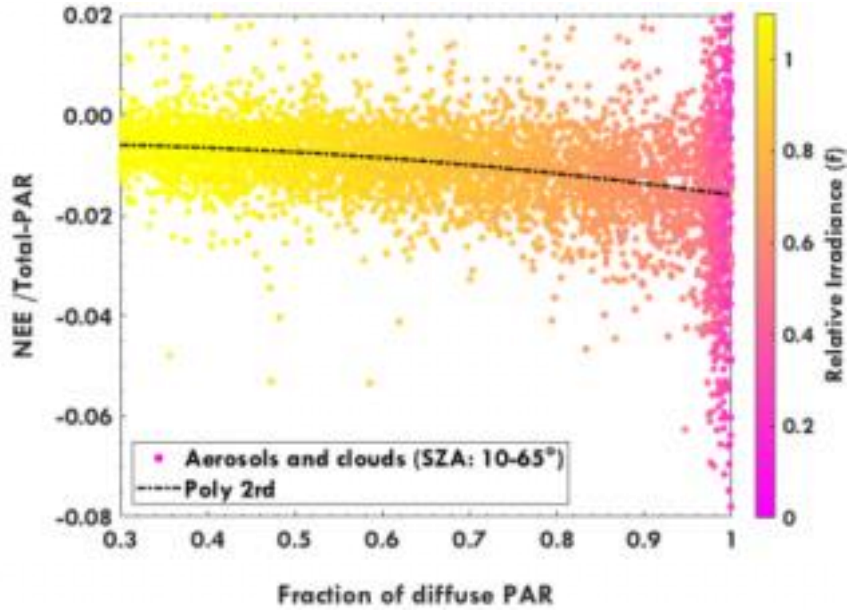

Source: Own figure

The pink and yellow colour represents the relative irradiance.

Figure 13 is the scatter plot that shows the relationship between NEE and PAR radiation flux. There is a non-linear relationship between the two variables, the highest values of PAR(t) are recorded at the lowest values of PAR radiation flux. In contrast, the highest values of diffuse PAR are recorded at the highest values of PAR differential flux, but the lowest values of PAR(t) and PAR (diff) were recorded between the average values of PAR radiation flux. The NEE's highest value of -40μmol^{-2}s^{-1} recorded at the highest values of radiation flux of 1000μmol/m^2.s.

We can observe a significant scattering of PAR (diff) at the lower values of PAR radiation flux and a significant scattering of PAR(t) at the high values of PAR radiation flux. These values were calculated at the solar azimuth angle between 10 and 35°.

Figure 13 - Scatter plot showing the Relative radiance from the relationship between NEE vs PAR radiative flux for ATTO.

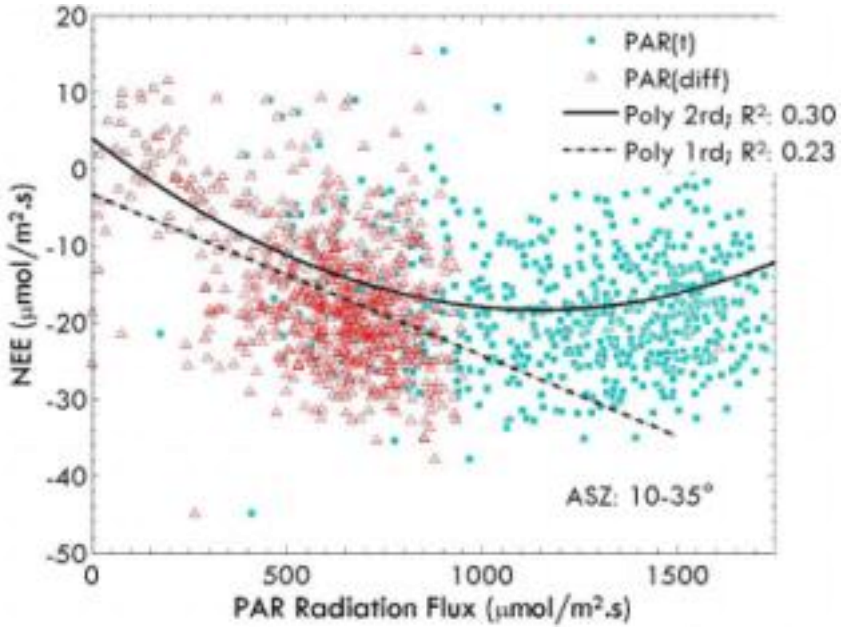

Source: Own figure

Figure 14 shows the box-plot of the relationship between the relative change in NEE (%) and the relative irradiance (f), with the highest values of relative change in NEE being in the 40th percentile at the values of relative irradiance of 0.8. The results are consistent with the results obtained by Cirino et al. (2014), this is where the maximum amount of carbon gets fixated, the maximum CO_2 fixation does not occur on a clear day (f ~1.0 and AOD < 0.10), but on days with either minimal cloud cover or moderate aerosol loading which increases the diffuse fraction of solar radiation. A calculated average increase of approximately 10 % in carbon uptake was observed relative to clear-sky (NEE_{csky}) conditions when the f is reduced from 1 to 0.8.

Figure 14 - Box plot for the relationship between the relative change in NEE(%) and radiative irradiance for ATTO.

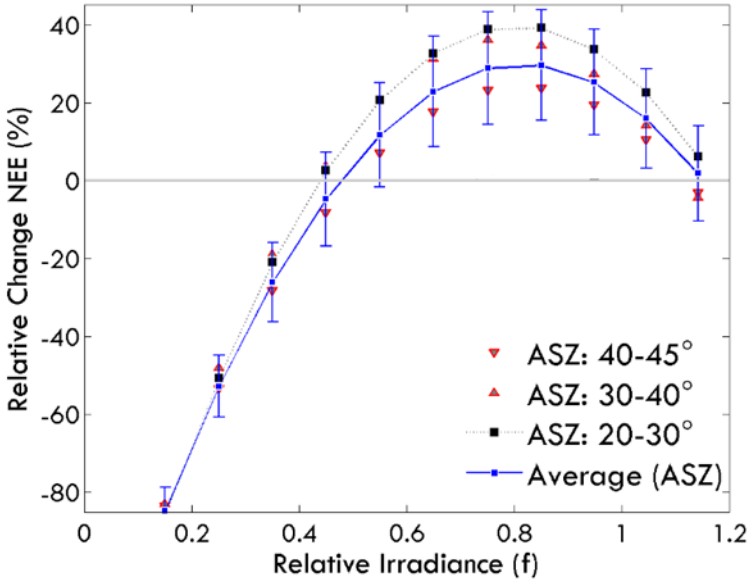

Source: Own figure

4.5Aerosols and cloud effects on temperature and VPD

The presence of clouds and aerosols can be both causes and consequences of changes in many atmospheric factors such as solar radiation, temperature, moisture, latent heating, and precipitation (GU et al., 2014). With reference to Cirino et al. (2014), there is a significant reduction in air temperature near the forest canopy and also in the vapor pressure deficit (VPD) associated with relative humidity, caused by the attenuation of incident solar irradiance due to the presence of aerosols and clouds. As analysed in this study, in figure 15, it can be observed that there is a decrease in air temperature as the number of clouds and aerosols increases, at values of relative irradiance between 0.8-1.5 Wm^2, and in consequence, this can cause the cooling of forest area.

Figure 15 - Relationship between the relative irradiance(f) and air temperature.

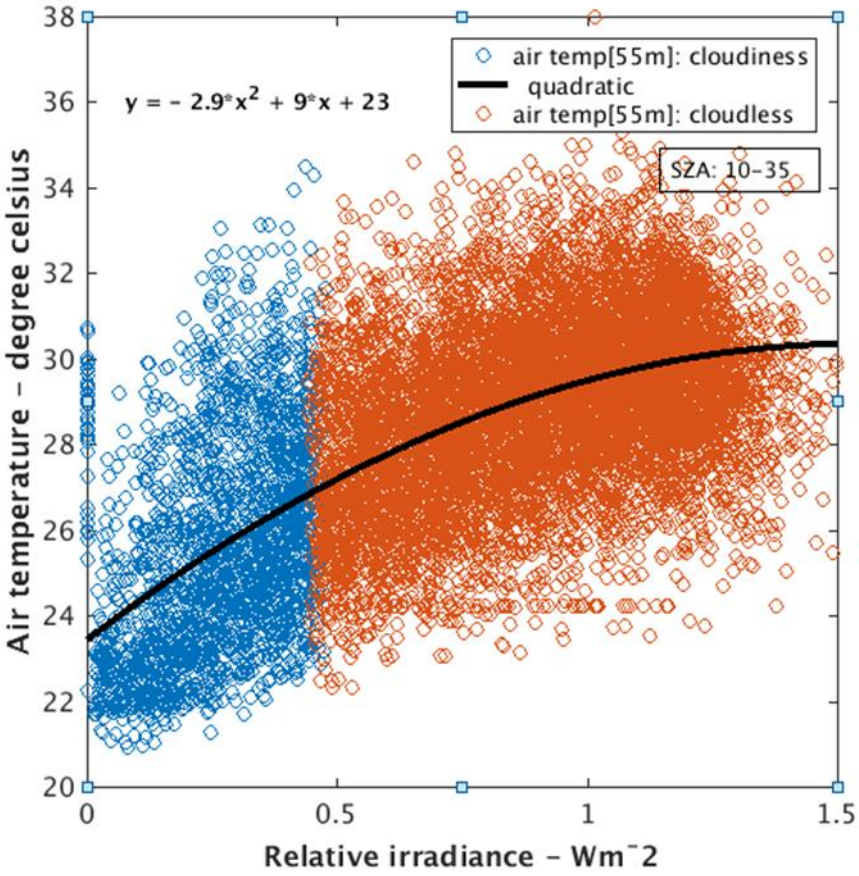

Source: Own figure

In figure 16, we have a scatter plot that shows the relationship between the canopy top temperature and relative irradiance. The same behaviour as the one observed with the air temperature can also be observed. There is a decrease in canopy top temperature with cloudiness and aerosols. Another factor that can increase canopy photosynthesis is the general trend of decreasing vapor pressure deficit on cloudy or smoke-filled skies (MIN & WANG, 2008). As shown in figure 17, which shows the relationship between VPD and relative irradiance (JING et al., 2010), attributed the reductions observed in the vapor pressure deficit to the reductions in air temperature in the forest canopy which can also be contributing to an increase in NEE. The general decreasing trends in VPD under cloudy and overcast conditions can induce stomatal openness and thus enhance leaf photosynthesis.

Figure 16 - Relationship between the relative irradiance(f) and canopy temperature.

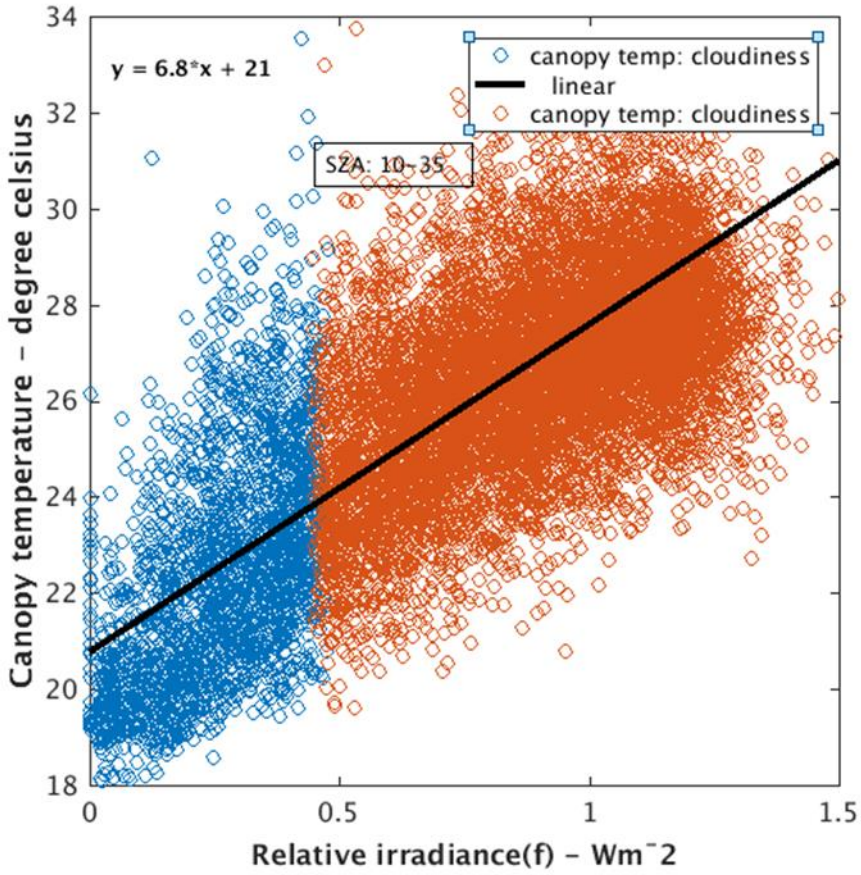

Source: Own figure

In studies such as by Oliphant et al. (2002), done in mixed hardwood forests, it was suggested that less direct influences on NEE include cooler leaf and soil temperatures under cloudy conditions which can lower respiration rates and decreases in vapor pressure deficit, enhancing stomatal openness

Figure 17 - Relationship between the relative irradiance (f) and VPD.

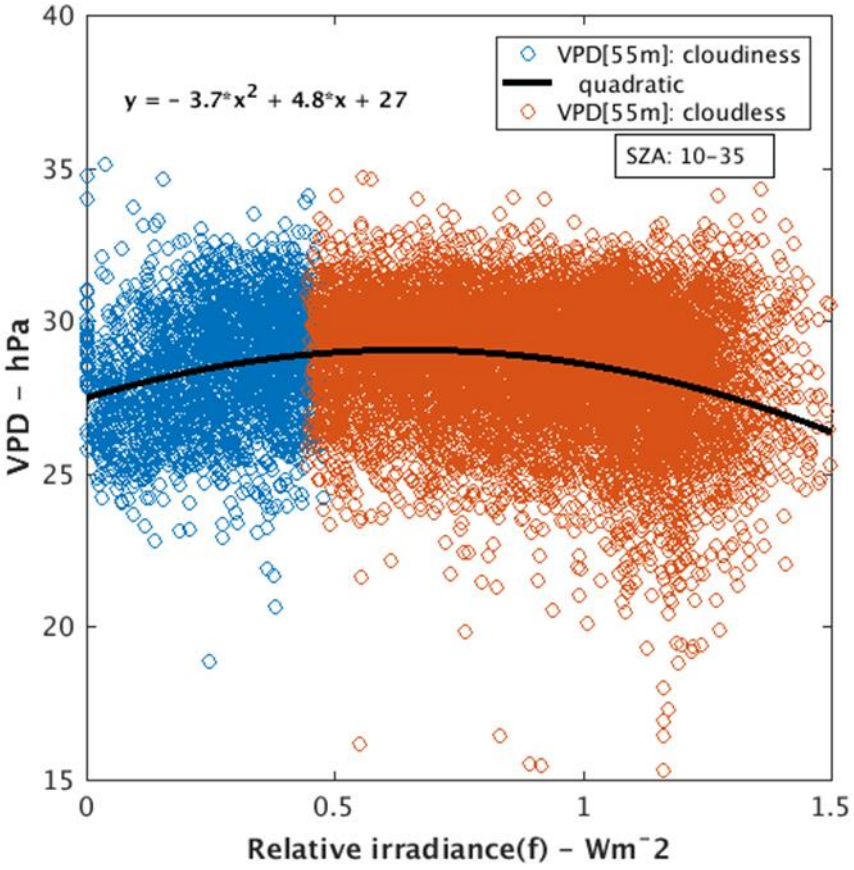

Source: Own figure

5 CONCLUSION

At ATTO, an average increase of 18 % and 25 % in the flux of CO2 and NEE was observed when the AOD values ranged from 0.10 to 0.30. The 18 and 25 % increase in NEE was attributed to an increase in the diffuse fraction of solar radiation concerning its direct fraction, mainly attributable to biogenic aerosols. Our observations indicate positive feedback between aerosols, clouds, and plant productivity as a response to the increased efficiency of light use in the ecosystem. Furthermore, the increase in NEE constitutes an effect of considerable relevance given the importance of carbon cycling in the Amazon.

Aerosol's particles may affect plant productivity through the increase in diffuse radiation fraction reaching the surface and, consequently, the Carbon cycle. The results have also shown that: clouds and aerosols cause a decrease in environmental factors such as air and canopy temperature as well as the vapor pressure deficit. A decrease in air temperature causes reduction in vapour pressure deficit which increases NEE and a decrease in the vapour pressure deficit, under cloudiness induces stomatal openness, which in the end increases photosynthesis.

REFERENCES

ANDREAE, M. O. *et al*. The Amazon tall tower observatory (atto): overview of pilot measurements on ecosystem ecology, meteorology, trace gases, and aerosols. **Atmospheric Chemistry and Physics**, Copernicus GmbH, v. 15, n. 18, p. 10723–10776, 2015.

ARAGAO, L. E.; POULTER, B.; BARLOW, J. B.; ANDERSON, L. O.; MALHI, Y.; SAATCHI, S.; PHILLIPS, O. L.; GLOOR, E. Environmental change and the carbon balance of Amazonian forests. **Biological Reviews**, Wiley Online Library, v. 89, n. 4, p. 913–931, 2014.

ARAUJO, A. de. *et al*. The spatial variability of co2 storage and the interpretation of eddy covariance fluxes in central Amazonia. **Agricultural and Forest Meteorology**, Elsevier, v. 150, n. 2, p. 226–237, 2010.

ARTAXO, P.; RIZZO, L. V.; BRITO, J. F.; BARBOSA, H. M.; ARANA, A.; SENA, E. T.; CIRINO, G. G.; BASTOS, W.; MARTIN, S. T.; ANDREAE, M. O. Atmospheric aerosols in amazonia and land use change: from natural biogenic to biomass burning conditions. Faraday discussions, **Royal Society of Chemistry**, v. 165, p. 203–235, 2013.

CIRINO, G.; SOUZA, R.; ADAMS, D.; ARTAXO, P. The effect of atmospheric aerosol particles and clouds on net ecosystem exchange in the amazon**. Atmospheric Chemistry and Physics**, Copernicus GmbH, v. 14, n. 13, p. 6523–6543, 2014.

COLLOW, A. B. M.; MILLER, M. A. The seasonal cycle of the radiation budget and cloud radiative effect in the amazon rain forest of Brazil. **Journal of Climate**, American Meteorological Society, v. 29, n. 21, p. 7703–7722, 2016.

ECK, T.; HOLBEN, B.; REID, J.; O'NEILL, N.; SCHAFER, J.; DUBOVIK, O.; SMIRNOV, A.; YAMASOE, M.; ARTAXO, P. High aerosol optical depth biomass burning events: A comparison of optical properties for different source regions. **Geophysical Research Letters**, Wiley Online Library, v. 30, n. 20, 2003.

ELTAHIR, EA; HAMPHRIES JR, EJ. The role of clouds in the surface energy balance over the amazon forest. **International Journal of Climatology: A Journal of the Royal Meteorological Society**, Wiley Online Library, v. 18, n. 14, p. 1575–1591, 1998.

GRIFFIN, R. J. The sources and impacts of tropospheric particulate matter. **Nature Education Knowledge**, Nature Education, v. 4, n. 5, p. 1, 2013.

GU, L.; BALDOCCHI, D.; VERMA, S. B.; BLACK, T.; VESALA, T.; FALGE, E. M.; DOWTY, P. R. Advantages of diffuse radiation for terrestrial ecosystem productivity. **Journal of Geophysical Research: Atmospheres**, Wiley Online Library, v. 107, n. D6, p. ACL–2, 2002.

GU, L.; FUENTES, J. D.; SHUGART, H. H.; STAEBLER, R. M.; BLACK, T. A. Responses of net ecosystem exchanges of carbon dioxide to changes in cloudiness: Results from two north American deciduous forests. **Journal of Geophysical Research: Atmospheres**, Wiley Online Library, v. 104, n. D24, p. 31421–31434, 1999.

HOLBEN, B. N. *et al*. Aeronet - a federated instrument network and data archive for aerosol characterization. **Remote Sensing of Environment**, Elsevier, v. 66, n. 1, p. 1–16, 1998.

HOUGHTON, R.; GLOOR, M.; LLOYD, J.; POTTER, C. The regional carbon budget. **Amazonia and Global Change, Geophys. Monogr**. Ser, v. 186, p. 409–428, 2009.

KIRSCHBAUM, M.; EAMUS, D.; GIFFORD, R.; ROXBURGH, S.; SANDS, P. Definitions of some ecological terms commonly used in carbon accounting. **Cooperative Research Centre for Carbon Accounting,** Canberra, p. 2–5, 2001.

KULMALA, M. *et al*. A new feedback mechanism ¨ linking forests, aerosols, and climate. **Atmospheric Chemistry and Physics**, Copernicus GmbH, v. 4, n. 2, p. 557–562, 2004.

LI, F. Quantifying the impacts of fire aerosols on global terrestrial ecosystem productivity with the fully-coupled earth system model cesm. **Atmospheric and Oceanic Science Letters**, Taylor & Francis, v. 13, n. 4, p. 330–337, 2020.

LIGHTY, J. S.; VERANTH, J. M.; SAROFIM, A. F. Combustion aerosols: factors governing their size and composition and implications to human health. **Journal of the Air & Waste Management Association**, Taylor & Francis, v. 50, n. 9, p. 1565–1618, 2000.

LOVETT, G. M.; COLE, J. J.; PACE, M. L. Is net ecosystem production equal to ecosystem carbon accumulation? **Ecosystems,** Springer, v. 9, n. 1, p. 152–155, 2006.

MAHOWALD, N.; WARD, D. S.; KLOSTER, S.; FLANNER, M. G.; HEALD, C. L.; HEAVENS, N. G.; HESS, P. G.; LAMARQUE, J.-F.; CHUANG, P. Y. Aerosol impacts on climate and biogeochemistry. **Annual review of environment and resources**, Annual Reviews, v. 36, p. 45–74, 2011.

MALAVELLE, F. F.; HAYWOOD, J. M.; MERCADO, L. M.; FOLBERTH, G. A.; BELLOUIN, N.; SITCH, S.; ARTAXO, P. Studying the impact of biomass burning aerosol radiative and climate effects on the amazon rainforest productivity with an earth system model. **Atmospheric Chemistry and Physics**, Copernicus GmbH, v. 19, n. 2, p. 1301–1326, 2019.

MALHI, Y.; BALDOCCHI, D.; JARVIS, P. The carbon balance of tropical, temperate and boreal forests. **Plant, Cell & Environment**, Wiley Online Library, v. 22, n. 6, p. 715–740, 1999.

MENDES, K. R. *et al*. Seasonal variation in net ecosystem co 2 exchange of a Brazilian seasonally dry tropical forest. **Scientific Reports**, Nature Publishing Group, v. 10, n. 1, p. 1–16, 2020.

MIN, Q. Impacts of aerosols and clouds on forest-atmosphere carbon exchange. **Journal of Geophysical Research: Atmospheres**, Wiley Online Library, v. 110, n. D6, 2005.

MYHRE, G.; MYHRE, C.; SAMSET, B.; STORELVMO, T. Aerosols and their relation to global climate and climate sensitivity. **Nature Education Knowledge**, v. 4, n. 5, p. 7, 2013.

NOBRE, C. A.; OBREGON, G. O.; MARENGO, J. A.; FU, R.; POVEDA, G. Características do clima amazônico: aspectos principais. **Amaz. Glob**. Chang, p. 149–162, 2009.

OLIPHANT, A. J.; SCHMID, H. P.; GRIMMOND, S.; SU, H.-B.; SCOTT, S.; VOGEL, C. 6.11 The role of cloud cover in net ecosystem exchange of co_2 over two mid-western mixed hardwood forests. *In*: CONFERENCE ON AGRICULTURAL AND FOREST METEOROLOGY, 25TH; JOINT CONFERENCE ON THE APPLICATIONS OF AIR POLLUTION METEOROLOGY WITH A & WMA, 12TH; FOURTH SYMPOSIUM ON THE URBAN ENVIRONMENT, 2002, Norfolk, Virginia. **Proceedings[**...**]**. Norfolk, Virginia: The Society, 2002. p. 77.

OLIVEIRA, L. G. B. de. *et al*. Analise do Sistema de coleta simultânea do perfil vertical de co_2 no pantanal mato-grossense. Universidade Federal de Mato Grosso, 2018.

OLIVEIRA, P. H.; ARTAXO, P.; PIRES, C.; LUCCA, S. D.; PROCOPIO, A.; HOLBEN, ´ B.; SCHAFER, J.; CARDOSO, L. F.; WOFSY, S. C.; ROCHA, H. R. The effects of biomass burning aerosols and clouds on the co2 flux in Amazonia. **Tellus B: Chemical and Physical Meteorology**, Taylor & Francis, v. 59, n. 3, p. 338–349, 2007.

PARAZOO, N. C. *et al*. Interpreting seasonal changes in the carbon balance of southern Amazonia using measurements of xco2 and chlorophyll fluorescence from gosat. **Geophysical Research Letters**, Wiley Online Library, v. 40, n. 11, p. 2829–2833, 2013.

PENNER, J. E. *et al*. Aerosols, their direct and indirect effects. In: **Climate change 2001**: the scientific basis. Contribution of working group I to the third assessment report of the intergovernmental panel on climate change. ***Proceedings[·]***. Cambridge University Press, 2001. p. 289–348.

SATURNO, J. *et al*. African volcanic emissions influencing atmospheric aerosols over the amazon rain forest. **Atmospheric Chemistry and Physics**, Copernicus GmbH, v. 18, n. 14, p. 10391–10405, 2018.

WU, L. *et al*. Single-particle characterization of aerosols collected at a remote site in the Amazonian rainforest and an urban site in Manaus, Brazil. **Atmospheric Chemistry and Physics**, Copernicus GmbH, v. 19, n. 2, p. 1221–1240, 2019.

ZHOU, H.; YUE, X.; LEI, Y.; TIAN, C.; MA, Y.; CAO, Y. Aerosol radiative and climatic effects on ecosystem productivity and evapotranspiration. **Current Opinion in Environmental Science Health**, v. 19, p. 100218, 2021. ISSN 2468-5844. Disponível em: <https://www.sciencedirect.com/science/article/pii/S2468584420300696>.

ZHU, P.; CHENG, S. J.; BUTTERFIELD, Z.; KEPPEL-ALEKS, G.; STEINER, A. L. The global influence of cloud optical thickness on terrestrial carbon uptake. **Earth Interactions**, v. 23, n. 6, p. 1–22, 2019.

ANNEXURE A – ADDITIONAL INFORMATIONS

Figure A1 - EGU poster

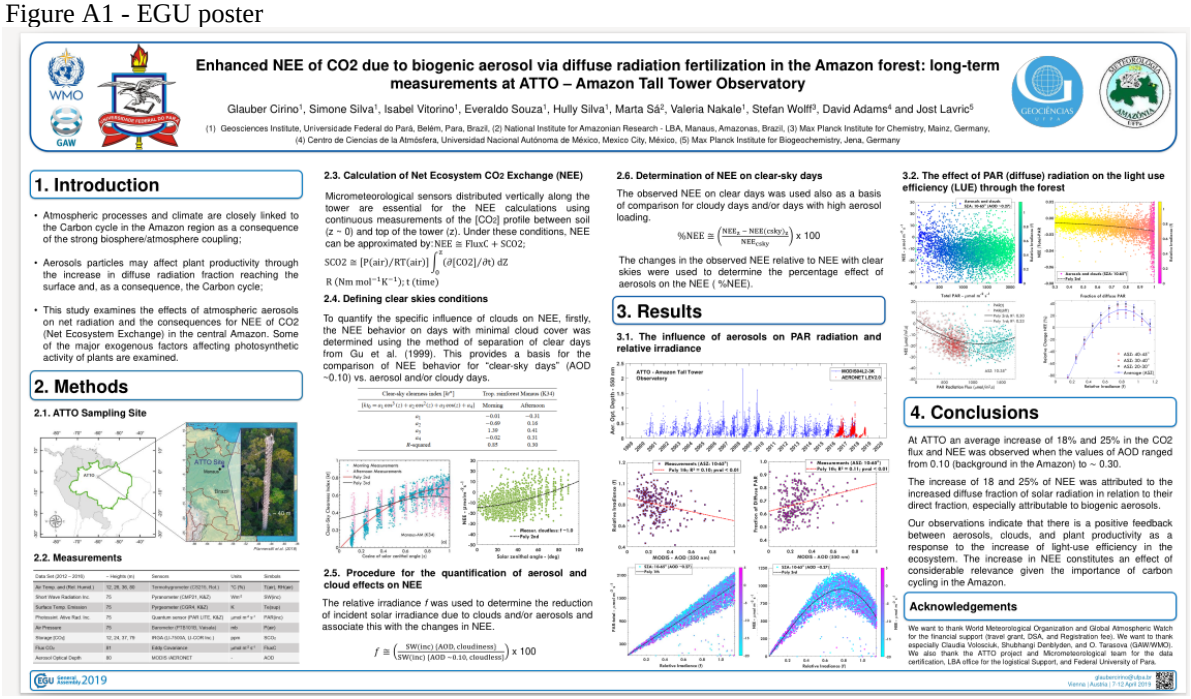

Figure A2 - EGU abstract

Geophysical Research Abstracts
Vol. 21, EGU2019-1710-5, 2019
EGU General Assembly 2019

Enhanced NEE of CO_2 due to biogenic aerosol via diffuse radiation fertilization in the Amazon forest: long-term measurements at ATTO – Amazon Tall Tower Observatory

Glauber Cirino (1), Simone Silva (1), Isabel Vitorino (1), Everaldo Bastos (1), Hully Silva (1), Marta Sá (2), Valeria Nakale (1), Stefan Wolff (3), David Adams (4), and Jost Lavric (5)

(1) Geosciences Institute, Universidade Federal do Pará, Belém, Para, Brazil (glaubercirino@ufpa.br), (2) National Institute for Amazonian Research, LBA, Manaus, Amazonas, Brazil (martasa.inpa@gmail.com), (3) Max Planck Institute for Chemistry, Mainz, Germany (stefan.wolff@mpic.de), (4) Centro de Ciencias de la Atmósfera, Universidad Nacional Autónoma de México, Mexico City, México (dave.k.adams@gmail.com), (5) Max Planck Institute for Biogeochemistry, Jena, Germany (jlavric@bgc-jena.mpg.de)

Atmospheric processes and climate are closely linked to the Carbon cycle in the Amazon region as a consequence of the strong biosphere/atmosphere coupling. Aerosols particles may affect plant productivity through the increase in diffuse radiation fraction reaching the surface and, as a consequence, the Carbon cycle. This study examines the effects of atmospheric aerosols on net radiation and the consequences for NEE of CO_2 (Net Ecosystem Exchange) in the central Amazon. Some of the major exogenous factors affecting photosynthetic activity of plants are examined. CO_2 flux and NEE are analyzed as a function aerosol concentration at the ATTO tower sampling site, located in the Uatumã Reserve, approximately 150 km northeast from Manaus in a pristine forest of the central Amazon. Remotely sensed Aerosol Optical Depth (AOD) measurements at 550 nm from the MODIS sensor on the Aqua and Terra platforms (MODIS Atmospheric Products, MOD/MYD04L2-3K, Collection 6.1), previously validated with AERONET (Aerosol Robotic Network) sun photometers. CO_2 fluxes are measured with fast-response eddy covariance method. An algorithm of clear-sky irradiance was developed from a long observational time series (2012-2016) to calculate a variable denominated relative irradiance f, used to express the amount of extinction solar radiation due to the presence of aerosols and clouds in the region. Overall net absorption of carbon by forest (NEE of CO_2) varied not only with the concentrations of aerosols, but also with cloud cover, solar elevation angle (SZA) and other parameters. At ATTO, an average increase of 18% and 22% in the CO_2 flux and NEE was observed when the values of AOD ranged from 0.10 (background in the Amazon) to ~ 0.50. For larger reduction in incident radiation the NEE was observed to be reduced to values close to zero. The increase of 18 and 22% of NEE was attributed to the increased diffuse fraction of solar radiation in relation to their direct fraction, especially attributable to biogenic aerosols. Important influences on the temperature and relative humidity induced by the interaction between radiation and high aerosol loading were also observed. In view of the transport of aerosols over long distances emitted by biomass burning, significant changes in the carbon flux may be occurring in large areas of Amazonia. The influence of aerosols on the CO_2 flux and NEE represents a very important effect for the Amazonian ecosystems and have an important influence on the global carbon budget.

Figure A3 - Regression coefficients of relationships between clear-sky irradiance (S0) and solar zenith angles cos(z) as well as relationships between clear-sky clearness index (kt*) and solar zenith angles cos(z) as well as relationships between clear-sky clearness index (kt*) and solar zenith angles cos(z) for the morning and afternoon periods of the K34 and RBJ sites. Periods of measurements: K34: 2000–2009 and RBJ: 2000–2002.

Regression coef.	Trop. rainforest Manaus (K34)		Trop. rainforest Ji-Parana (RBJ)	
	Morning	Afternoon	Morning	Afternoon
Clear-sky irradiance [S_0]				
$[S_0' = p_1\cos^3(z) + p_2\cos^2(z) + p_3\cos(z) + p_4]$				
p_1	−1026	−685	−813	−644
p_2	2027	1210	1867	1188
p_3	−110	240	−170	295
p_4	10	14	11	18
R-squared	0.95	0.85	0.95	0.92
Clear-sky clearness index [kt^*]				
$[kt_0 = a_1\cos^3(z) + a_2\cos^2(z) + a_3\cos(z) + a_4]$				
a_1	−0.01	−0.31	−0.14	−0.54
a_2	−0.69	0.16	−0.29	0.63
a_3	1.39	0.41	1.13	0.13
a_4	−0.02	0.31	−0.04	0.41
R-squared	0.85	0.30	0.87	0.41

Source: Cirino et al. (2014).

Figure A4 - Scatter plots and regressions between clear-sky clearness index and the cosine of solar zenith angle for the K34 site near Manaus (2000–2009) (a)and for the RBJ site in Ji-Parana (2000–2002) (b).

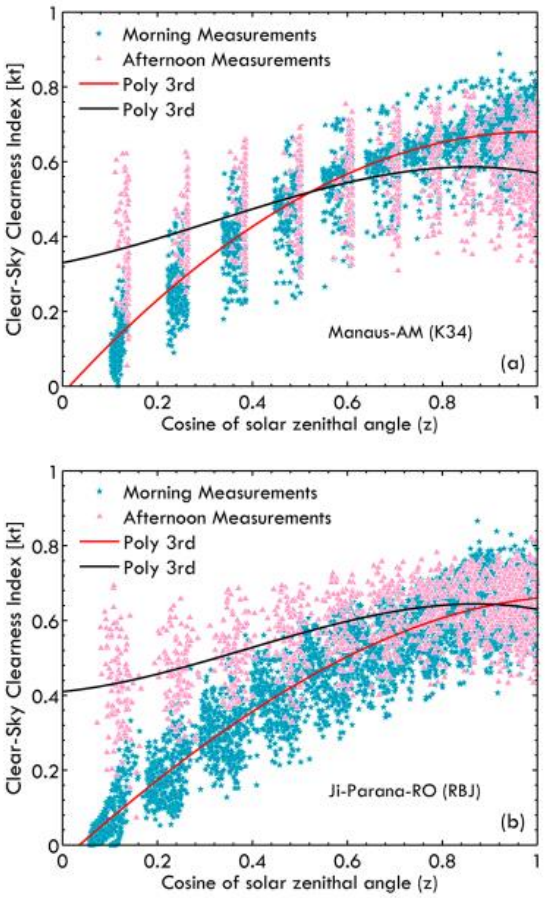

Source: Cirino et al. (2014).

Figure A5 - Relationship between NEE and solar zenith angle (SZA) for clear-sky conditions (f=1.0) at K34(a)for a poly 2nd fit with R2=0.27 and p<0.01, and at the RBJ(b)for a 2nd order polynomial fit with R2=0.60 and p<0.001.

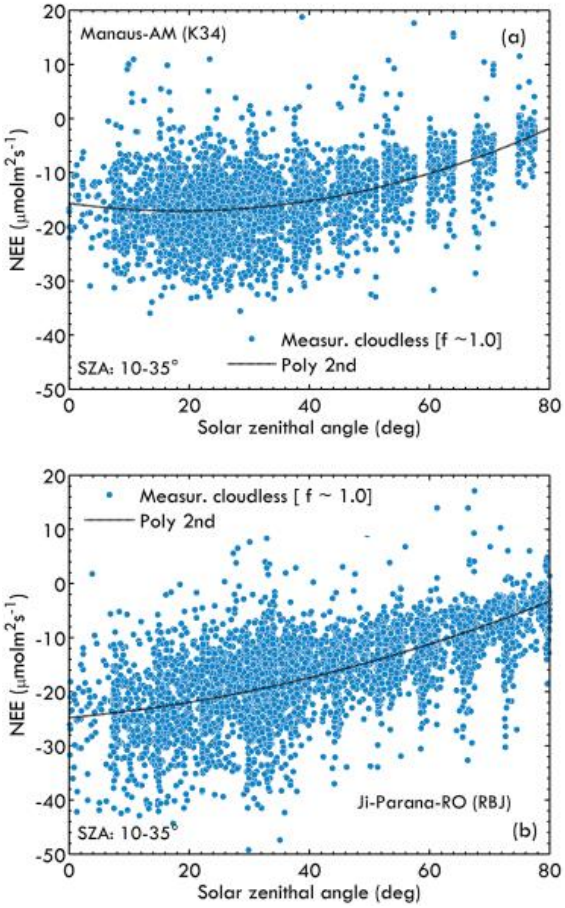

Source: Cirino et al. (2014).

Figure A6 - Regression coefficients of relationship between NEE and solar zenith angle (SZA) for clear-sky conditions (f1.0) observed during the year at the K34 and RBJ sites. The fitted equation is NEE=n3+n2(SZA)+n1(SZA)2.

Measurements (morning) Clear-sky	Regression of parameters			
	n_1^*	n_2^*	n_3^*	*R*-squared
Trop. Rainforest (RBJ)/2000–2002				
NEE of CO_2-μmol m^{-2} s^{-1}	0.002	0.100	−24.8	0.60
Trop. Rainforest (K34)/2000–2009				
NEE of CO_2-μmol m^{-2} s^{-1}	0.004	−0.152	−15.7	0.27

* *n* indicates coefficients of the regression curve (Fig. 3).

Source: Cirino et al. (2014).